PROOF-OF-PRINCIPLE EXPERIMENTAL DESIGN OF SOLENOID-BASED RELATIVISTIC ELECTRON BEAM PULSE COMPRESSION

Ch. Shi, H. Zha*, H. Chen, J. Shi, An Li, W. Huang, Tsinghua University, Beijing, China

Abstract

Relativistic electron beam pulse compression can enhance the beam current intensity within the pulse and generate higher peak current, showing significant potential for applications such as FLASH radiotherapy and wakefield acceleration. This paper proposes a proof-of-principle experimental design for a solenoid-based electron beam pulse compression scheme. The core device of the experiment, namely the magnetic compressor, has an approximately cylindrical structure with a diameter of 42 cm and a height of 47 cm. By utilizing the uniform magnetic field generated by the solenoids, the compressor converts the energy difference of the injected beam bunch into a path-length difference to achieve pulse compression. Simulation studies show that, under a transverse geometric emittance of 10 mm · mrad, the beam loss remains below 10 %, while the output current waveform exhibits a peak-to-peak ratio of approximately 5, demonstrating an obvious pulse compression effect.

INTRODUCTION

In accelerator physics, high-current high-energy electron beams are not only important subjects of research but also key tools for a wide range of applications. For example, in FLASH radiotherapy [1], they have the potential to achieve efficient tumor irradiation while providing better protection for normal tissues. In two-beam acceleration schemes [2], they can be used to enhance the wakefield gradient generated by the drive beam. However, due to the pronounced relativistic effects of high-energy electron beams, whose particle velocities approach the speed of light, it is difficult to achieve effective bunch compression solely through energy modulation and the resulting velocity modulation. Consequently, realizing short pulse durations and high peak beam currents remains a significant challenge.

In contrast, exploiting the dispersive properties of electron beams in magnetic fields to manipulate particle trajectories, thereby directly converting energy modulation into path-length modulation for bunch compression, provides a more effective approach. GELINA [3] is a representative facility that achieves electron bunch compression based on this principle. However, the compression magnet in GELINA relies on a relatively large energy chirp, resulting in a bulky system and limited compression scalability, which restricts its broader application and further development.

In this work, a proof-of-principle experimental scheme for electron bunch compression based on a solenoidal magnetic field is proposed. In this scheme, the electron beam propagates along helical trajectories generated by the solenoidal field, with the beam path tightly confined and folded within a finite cylindrical volume. Compared with conventional compression structures, the proposed scheme requires only a compact cylindrical device while still providing a sufficiently long propagation path for beam compression, thereby significantly improving space utilization efficiency.

* zha_hao@mail.tsinghua.edu.cn

PRINCIPLE AND EXPERIMENTAL DESIGN

Magnetic Compression Principle

Assume that there exists a uniform magnetic field B_0 along the axial z direction. When the electron velocity is neither perpendicular nor parallel to the magnetic field, the electron performs helical motion around the magnetic field direction, as shown in Fig. 1.

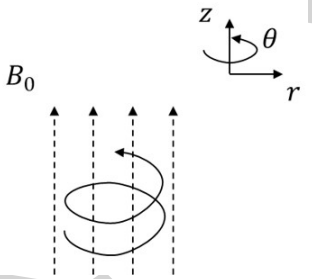

Figure 1: Helical motion of electrons in a solenoid magnetic field.

The equations of motion can be written as

$$\frac{dz}{dt} = v_z \tag{1}$$

$$\frac{d\theta}{dt} = \frac{eB_0}{\gamma m_e} \tag{2}$$

where e is the electron charge, $\gamma = E/(m_e c^2)$ is the Lorentz factor, m_e is the electron rest mass, and E is the electron energy.

When two electrons have the same propagation direction but different energies, Eq. (2) indicates that their angular velocities in the helical motion become different. Consequently, the path-length difference in the θ direction between electrons with different energies continuously accumulates during propagation. When the axial velocity component v_z is much smaller than the azimuthal velocity component v_θ, the path-length difference in the θ direction can be approximately regarded as the effective compression distance, thereby enabling longitudinal compression of the electron beam.

However, when the condition $v_z \ll v_\theta$ is no longer satisfied, or when the propagation distance becomes excessively

long, electrons may gradually separate along the axial direction, which weakens the compression effect. In such cases, additional axial focusing elements are generally required to maintain bunch confinement. For the proof-of-principle experiment proposed in this work, no additional axial focusing structure is introduced in order to reduce the complexity of the experimental system. Instead, the influence of axial beam spreading is minimized through parameter optimization.

Magnetic Compressor Design

The structure of the magnetic compressor is shown in Fig. 2. Both the main coil and the auxiliary coils are made of copper, while the shell, injection tube, extraction tube, and iron core are fabricated from 1008 steel. The main structural dimensions of the magnetic compressor are listed in Table 1.

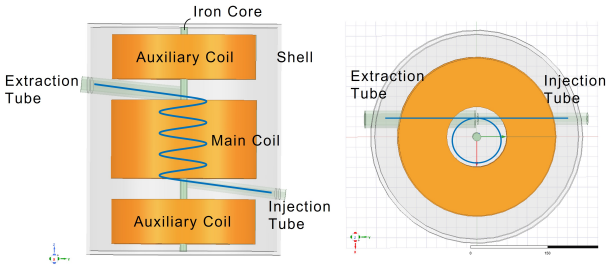

Figure 2: Structure of the magnetic compressor. The electron trajectory is illustrated by the blue solid line.

Table 1: Main Structural Parameters of the Magnetic Compressor

Parameter	Value
Overall diameter	42 cm
Overall height	47 cm
Upper and lower auxiliary coils	
Thickness	96 mm
Inner radius	60 mm
Outer radius	156 mm
Current	47625 A
Central main coil	
Thickness	169 mm
Inner radius	70 mm
Outer radius	158 mm
Current	38473 A
Injection tube	
Length	220 mm
Inner radius	6 mm
Outer radius	8 mm
Angle with XOY plane	7.153 deg
Extraction tube	
Length	220 mm
Inner radius	12 mm
Outer radius	17.5 mm
Angle with XOY plane	5.582 deg

Experimental Layout

The schematic layout of the experiment is shown in Fig. 3. The system employs two RF power sources, M_1 and M_2, with frequencies of f_1 and $f_1 - \Delta f$, respectively, to provide accelerating fields for two separate accelerating structures.

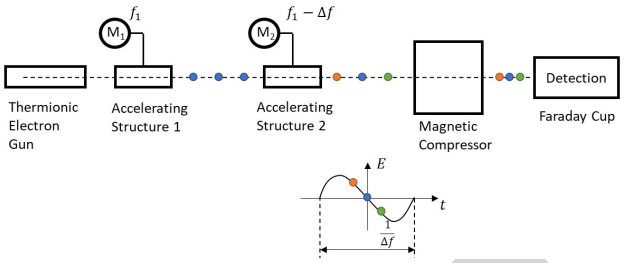

Figure 3: Schematic layout of the experiment.

After passing through the first accelerating structure, the electron beam forms a bunch train with a repetition frequency of f_1. Since the RF frequency in the second accelerating structure differs from the bunch repetition frequency by Δf, the bunches gradually experience phase slippage with respect to the RF field while propagating through the second structure. As a result, different bunches experience accelerating fields with different RF phases, as illustrated by the orange dots in Fig. 4, thereby generating a periodic energy modulation within the bunch train.

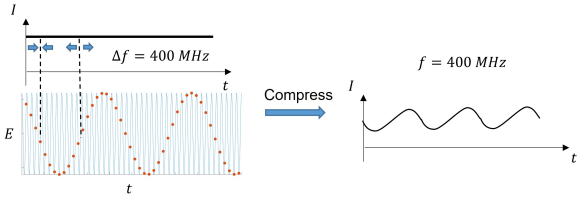

Figure 4: Illustration of RF phase slippage and energy modulation in the second accelerating structure.

The energy-modulated bunch train then passes through the magnetic compressor. During the compression process, electrons with different energies gradually accumulate path length differences, which are subsequently converted into spatial density modulation. The compressed beam is finally measured by a detector. If the detected beam current frequency matches the difference frequency Δf between the two RF power sources, it demonstrates that the magnetic compressor has successfully converted the energy modulation into spatial density modulation, thereby validating the proposed compression mechanism.

BEAM DYNAMICS SIMULATION

The beam parameters used in the dynamics simulation are listed in Table 2. The injection tube serves as a magnetic shielding structure, allowing the electrons to maintain nearly straight-line motion before entering the uniform magnetic-field region. Similarly, the extraction tube guides the electrons out of the uniform-field region after compression. A schematic illustration of the electron trajectory is shown by the blue solid line in Fig. 2.

Table 2: Beam and RF Parameters Used in the Dynamics Simulation

Parameter	Value
Transverse emittance	10 mm·mrad
Bunch energy spread	3%
Central beam energy	3.0 MeV
Energy modulation amplitude	0.4 MeV
Bunch length	6.3 mm
RF frequency f	9.3 GHz
Frequency difference Δf	400 MHz

The injection and extraction current profiles are shown in Fig. 5. The simulation results show that 96.14 % of the particles can be successfully extracted through the extraction tube, indicating that the proposed magnetic compressor is capable of achieving electron beam compression while maintaining high transmission efficiency. In addition, the extracted current waveform exhibits a peak-to-peak ratio of approximately 5, demonstrating a clear pulse compression effect. Preparations for the subsequent experimental study are currently underway.

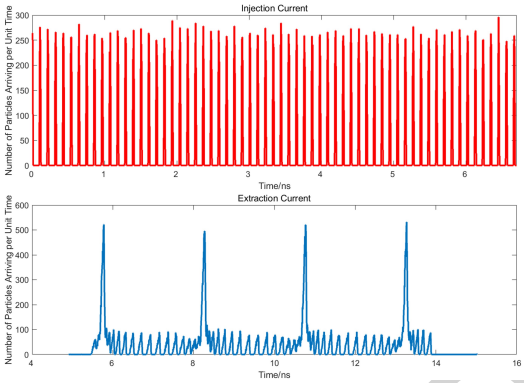

Figure 5: Temporal distributions of the injection and extration currents.

CONCLUSION

A proof-of-principle experimental scheme for solenoid-based relativistic electron beam pulse compression has been proposed. By utilizing the helical motion of electrons in a solenoidal magnetic field, the scheme converts beam energy modulation into path-length modulation within a compact cylindrical structure.

A corresponding experimental layout based on dual-frequency RF acceleration was designed to generate periodic energy modulation in the electron bunch train. Particle dynamics simulations demonstrate that the proposed magnetic compressor can achieve effective beam pulse compression while maintaining high transmission efficiency. Under the present simulation conditions, 96.14 % of the particles can be successfully extracted through the compression structure, and the extracted beam current exhibits clear current enhancement after compression.

The results indicate the feasibility of the proposed compression mechanism and provide a foundation for future experimental verification and further optimization of the compression performance.

REFERENCES

[1] B. Lin, F. Gao, Y. Yang *et al.*, "FLASH Radiotherapy: History and Future", *Front. Oncol.*, vol. 11, p. 644400, 2021. doi:10.3389/fonc.2021.644400

[2] J. Shao, C. Jing, S. Antipov *et al.*, "Recent Two-Beam Acceleration Activities at Argonne Wakefield Accelerator Facility", in *Proc. IPAC'17*, Copenhagen, Denmark, May 2017, pp. 3305–3307. doi:10.18429/JACoW-IPAC2017-WEPVA022

[3] A. Bensussan and J. Salome, "GELINA: A Modern Accelerator for High Resolution Neutron Time of Flight Experiments", *Nucl. Instrum. Methods*, vol. 155, no. 1, pp. 11–23, 1978. doi:10.1016/0029-554X(78)90181-7